Alignment, Morphology and Defect Control of Vertically aligned ZnO Nanorod array: Competition between 'surfactant' and 'stabilizer' roles of the amine species in aqueous solution growth

Kugalur Shanmugam Ranjith,[a] Ramanathaswamy Pandian,[b] Enda McGlynn[c] and Ramasamy Thangavelu Rajendrakumar*[a, d]

Abstract

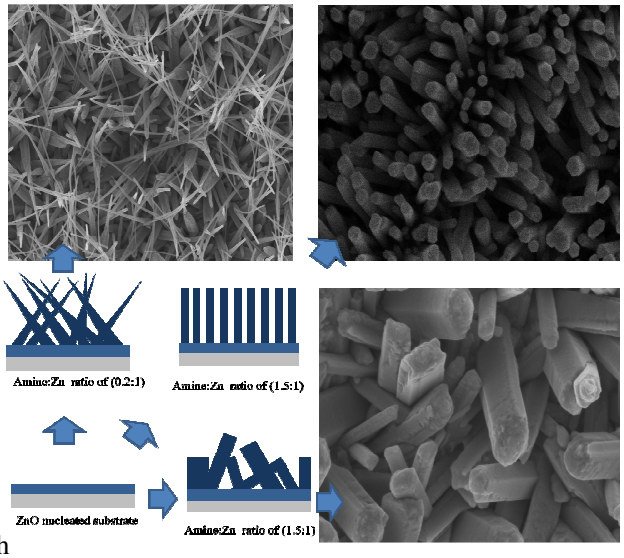

We show that the morphology, defect and alignment of vertically aligned one dimensional (1D) ZnO nanorod (NR) arrays grown using an aqueous solution method could be effectively controlled by simply varying the hexamine concentration in the growth solution. Lower amine concentration (0.2 M) resulted in randomly aligned ZnO NRs with non uniform diameters. Increasing the amine concentration (to 1.0 M) yielded well aligned, prismatic ZnO NR arrays with uniform NR diameters of 80 nm along the NR length. 1D growth ceases on further increasing the amine concentration (> 1M) and this favors the formation of 2D platelet like structures. Contact angle (CA) measurements show increases in CA from 83º to 145º with increases in amine concentrations due to improvement in alignment of the ZnO NR array. Low temperature (10 K) photoluminescence studies revealed that increases in amine concentration (0.2 to 1M) increases the optically active defect concentration and influences both free and bound exciton emissions from ZnO NRs. Investigations revealed that the amine acts both as a growth stabilizer and a surfactant and thus controls both Zn release for ZnO formation and caps non-polar planes, the latter function facilitating 1D anisotropic grown along the [002] direction. The competition between the 'stabilizer' and 'surfactant' roles by the amine facilitates the morphology, alignment and defect control of 1D ZnO NR array. At low amine concentrations, the role as surfactant dominates over that of stabilizer which does not favor uniform growth due to the slow release of Zn to form ZnO. On increasing the amine concentration, Zn release and amine capping aspects balance and this results in uniform and aligned growth of NR arrays. At the higher amine concentrations, the sudden release of Zn generates an overshoot effect, which dominates over the surfactant capping aspect, thus favoring the growth of irregular micro platelets.

Understanding the role of amine in the growth of 1D ZnO NR arrays holds great promise for tailoring ZnO NR functionalities for various potential applications.

Alignment, Morphology and Defect Control of Vertically aligned ZnO Nanorod array: Competition between 'surfactant' and 'stabilizer' roles of the amine species and its Photocatalytic properties

Kugalur Shanmugam Ranjith,[a] Ramanathaswamy Pandian,[b] EndaMcGlynn[c] and Ramasamy Thangavelu Rajendra kumar*[a, d]

[a]Advanced Materials and Devices Laboratory, Department of Physics, Bharathiar University, Coimbatore, India. *Fax: (91)422-2422387Tel: 9894865562; E-mail: rtrkumar@buc.edu.in*

[b] *Surface and Nanoscience Division, Materials Science Group, IGCAR, Kalpakkam, India. Fax:(91)42-27480081; Tel: (91) 44 27480500; E-mail: ramanathaswamy@gmail.com*

[c]*School of Physical Sciences, National Centre for Plasma Science & Technology, Dublin City University, Glasnevin, Dublin 9, Ireland. Fax: ++353 1 7005384; Tel: ++353 17005387; E-mail: enda.mcglynn@dcu.ie*

[d] *Department of Nanoscience and Technology, Bharathiar University, Coimbatore, India. Fax: (91)422-2422387; Tel: 9789757888; E-mail: rtrkumar@buc.edu.in*

Abstract

We show that the morphology, defect and alignment of vertically aligned one dimensional (1D) ZnO nanorod (NR) arrays grown using an aqueous solution method could be effectively controlled by simply varying the hexamine concentration in the growth solution. Lower amine concentration (0.2 M) resulted in randomly aligned ZnO NRs with non-uniform diameters. Increasing the amine concentration (to 1.0 M) yielded well aligned, prismatic ZnO NR arrays with uniform NR diameters of 80 nm along the NR length. 1D growth ceases on further increasing the amine concentration (> 1M) and this favors the formation of 2D platelet like structures. Contact angle (CA) measurements show an increase in CA from 83º to 145º with an increase in amine concentrations due to improvement in alignment of the ZnO NR array. Low temperature (10 K) photoluminescence studies revealed that increase in amine concentration (0.2 to 2M) increases the optically active defect concentration and influences both free and bound exciton emissions from ZnO NRs. Investigations revealed that the amine acts both as a growth stabilizer and a surfactant and thus controls both Zn release for ZnO formation and caps non-polar planes, the latter function facilitating 1D anisotropic grown along the [002] direction. The competition between the 'stabilizer' and 'surfactant' roles by the amine facilitates the morphology, alignment and defect control of 1D ZnO NR array. At low

amine concentrations, the role as surfactant dominates over that of stabilizer which does not favor uniform growth due to the slow release of Zn to form ZnO. On increasing the amine concentration, Zn release and amine capping aspects were balanced and this result in uniform and aligned growth of NR arrays. At the higher amine concentrations, the sudden release of Zn generates an overshoot effect, which dominates over the surfactant capping aspect, thus favoring the growth of irregular micro platelets. 1D, well aligned, prismatic, ZnO NR arrays grown at an amine concentration of 1M show higher photocatalytic degradation activity for the degradation of Methylene Blue dye solution under UV irradiation owing to both the high surface to volume ratio of the arrays and increased charge carrier density due to Zn interstitial defects. Zinc interstitials are shallow donors readily supply electrons to conduction band which could buildup space charge near to the nanocatalayst surface. The occurrence of band bending associated with the interfacial electric field in the space charge region could facilitate the separation of photogenerated electrons and holes and thus enhances the photocatalytic performance. Understanding the role of amine in the growth of 1D ZnO NR arrays holds great promise for tailoring ZnO NR functionalities for various potential applications

Introduction

ZnO is an environmentally friendly and nontoxic II-VI semiconducting material possessing a high exciton binding energy of 60meV and a wide band gap of ~ 3.3eV. Recently, researchers have shown tremendous interest in 1D ZnO nano arrays due to their remarkable physical and chemical properties [1]. 1D ZnO nanostructural arrays have been extensively studied due to their potential applications in nanodevices such as sensors [2], solar cells [3], light emitting diodes [4], field effect transistors [5] and field emitters [6].These nanostructures have large surface area, high aspect ratio, and show quantum confinement and high electron mobility compared to nanoparticle thin films. Synthesis of well aligned 1D nanostructured arrays is of great interest because it is an important step towards realizing nano-optoelectronics devices, which include light emitting diodes and laser diodes. Many techniques are used to produce vertically aligned 1D ZnO nanostructural arrays, including vapour phase transport [7], metal organic vapour phase transport [8], thermal evaporation [9], pulsed laser deposition [10], spray pyrolysis[3], electro chemical deposition [11], hydrothermal [12] and aqueous solution technique [13]. Among the many methods reported for the growth of ZnO nanostructures, the aqueous solution technique is simple, cost effective and nanostructures can be obtained at lower growth temperature, thereby facilitating growth on a wide range of possible substrates with a reduced cost in terms of process steps. As mentioned above, morphology and defect control of ZnO

nanoarrays are important for their applications in optoelectronics. Very few authors have used hexamine as a surfactant along with growth precursors to control the morphology of ZnO nanostructures in aqueous solution growth. Control of defects in ZnO nanostructures is also critical for their applications in optoelectronics. Jingbiao Cui et al.,[11] has reported no role due to amine in the growth solution for the growth of ZnO structures via electrodeposition. Other reports show that defect emission from ZnO nanostructures may be controlled by plasma treatment of nanostructures [14]. Besides plasma treatment, annealing processes in various gas ambients (i.e., O_2, H_2, N_2, etc.) conditions is also useful for controlling the defect concentration in nanorods [15, 16]. Control on the defect state play a major role on tune the optoelectronic properties of nanostructures. Rapid progress in nanotechnology promises few semiconductors as a potential tool on the environmental remediation applications. Semiconductors such as titanium dioxide (TiO_2), zinc oxide (ZnO), iron oxide (Fe_2O_3), tungsten oxide (WO_3) and cadmium sulphide (CdS) have became popular as a photocatalyst for degradation of organic pollutance in water and air. Recently the ZnO based nanostructures has attracted much attention as a photocatalysis on removing the organic dye pollutance from the water. Although the photocatalytic activity of the ZnO nanostructures toward the organic molecules have been widely documented, studies on their renewable catalytic properties are rarely performed and presumably because of the poor recovery of the catalyst for multiple use [17, 18, 19]. Recovery of the ZnO powders after photocatalytic water treatment is tricky/complex but a necessity. Due to the cost of recovery operations, possible powder loss and to avoid the catalysis presence in the degraded solution after purification, it is proposed that instead of ZnO nano powders, ZnO nanostructural arrayed thin films may be used. For water treatment applications, ZnO nanoarrays might be interesting as dispersion of the catalyst and the catalyst loss will be avoided.

In this work, we highlight the effects of varying hexamine concentration in the precursor-solution on the growth, morphology and alignment control of ZnO nanorod arrays. We show that increase in hexamine concentration drastically affects the morphology and defect content of ZnO nanostructures. On increasing the hexamine concentration, the aspect ratio of ZnO nanorods decreases along while the optically active defect concentration increases, associated with an increased release rate of Zn ions in growth solution. We demonstrate that well aligned ZnO NR arrays show higher photocatalytic activity. And we propose that amine concentration not only plays an important role on the growth and alignment of the 1D NR arrays, but it also plays a role in the control of their the defect states and improved the photocatalytic efficiency.

Materials and Methods

ZnO nanostructures were synthesized by a low temperature aqueous solution growth method. A ZnO buffer layer of ~100 nm thickness was coated on glass substrates by dip coating method [20]. For the growth solution, zinc nitrate hexahydrade $Zn(NO_3)_2.6H_2O$ and hexamine (HMTA) ($C_6H_{12}N_4$) were dissolved in double distilled water and stirred continuously for 15 min in separate beakers. HMTA solution was added drop wise to $Zn(NO_3)_2$ solution and stirred continuously for 20 min to form a single phase solution. The buffer layer coated substrates were immersed in the growth solution and maintained at 90°C for 4 hours. After completing the growth process, the substrates with deposited nanostructures were cleaned twice, with distilled water and ethanol, and baked at 150°C. The molar ratio between the hexamine and zinc nitrate hexahydrade was varied with the ratios, (0.2:1), (0.5:1), (0.75:1), (1:1), (1.5:1) and (2:1). X-ray diffraction was used to investigate the crystalline phase of ZnO nanostructures (Bruker Advanced D8). Plane and cross-sectional images of ZnO nanostructural arrays were obtained using a field-emission scanning electron microscopy (FESEM). The photoluminescence (PL) properties of the synthesised nanostructural arrays were investigated by generating 325-nm line of a HeCd laser operating in the range 80 - 200 mW. The spectra were recorded at temperatures in the range 10 K using Janis closed cycle helium cryostats. The luminescence was analysed by a SPEX 0.75 m grating spectrometer equipped with a LN2-cooled Jobin-Yvon CCD detector for the radiotracer implanted samples, and a Jobin-Yvon iHR320 grating spectrometer fitted with an Andor Newton EM-CCD detector cooled to -25°C for the uniaxial stress and normal PL measurements.

Photocatalytic degradation

The photocatalytic activity of the ZnO NR arrays was evaluated using a 9 W of Hg lamp (ZF-1 UV, Philips, China), setup with strongest emission at ~365nm. The amine:Zn ratio controlled ZnO NR arrays of dimension 4 cm x 1 cm were immersed in 5 ml of 15 ppm Methylene Blue (MB) dye solution in a typical quartz container. Quartz container with samples grown with different amine ratios were placed side by side at the same time and irradiated under UV light at a distance of 10 cm to minimize heating effects. The catalyst loaded solution was first kept in the dark for 10 minutes to achieve an absorption/desorption equilibrium between the catalyst and the MB dye molecules. After UV irradiation the substrate was removed and the dye solution was collected and UV-Vis absorption analyses were performed using a JASCO V-660 spectrophotometer. After these spectral measurements, the substrates were placed back into the solutions for further irradiation for periods of 20 min (at which time further UV-Vis absorption analyses were performed) for 200 min in total. The

concentration of organic dyes was determined by measuring the absorption intensity at the maximum absorbance wavelength of the supernatant (for MB = 661 nm). The degradation percentage (η) of the solutions is defined as follows [21].

$$\eta = \frac{C_0 - C_t}{C_0} \times 100$$

C_o is the initial dye concentration and C_t the dye concentration after an illumination time t (min).

Result and Discussion

Figure 1 shows SEM images of the ZnO nanostructures grown using different amine: zinc nitrate ratios and the corresponding growth schematic are shown in figure 2. A low amine: Zn concentration ratio of (0.2:1) results in randomly aligned ZnO 1D nanostructures (figure 1a, figure 2a). The diameter of the nanorods at their base is around 150 - 200 nm and decreased to 30 nm at their top. On increasing the hexamine:Zn ratio to (0.5:1), the alignment of nanorod arrays improved (figure 1b) and the diameter was again found to gradually from their base (100 – 150 nm) to the top (30 nm). Figure 1c shows the morphology of nanorod arrays grown with amine:Zn ratio of 0.75:1. At this growth condition, the alignment of the nanorod arrays was further improved and the diameters of the NRs were nearly constant along their length. By increasing the amine:Zn to 1:1 better control over the morphology and alignment of the NRs was achieved (Fig. 1d) and well aligned, homogenously distributed and clearly faceted hexagonal NRs with diameters of 80nm were obtained. Further increasing the amine:Zn concentration to 1.5:1 resulted in NRs with an inhomogeneous morphology and diameters (50-150 nm) as shown in figure 1e. Finally, increasing the amine:Zn concentration to 2:1 resulted in the formation of two dimensional nanostructures with platelet/disc-like morphology (figure 1f).

Figures 3a, 3b & 3c show the cross sectional views of ZnO nanorod arrays grown at amine:Zn ratios of 0.2:1, 1:1 and 1.5:1, respectively. The concentration of amine plays a critical role on the control of NR length and the diameter of the nanostructures. On increasing the amine concentration in the growth solution, the diameter of the NRs increased along with a decrease in the length of the NRs (Table I). Figure 4 shows the XRD patterns from ZnO nanostructures prepared with different concentration ratios of amine:Zn. The observed XRD peaks match well with those predicted for wurtzite ZnO (JCPDS card 36-1451) in all cases (figure 4a). Figure 4b indicates the presence of (100), (002) and (101) peaks from ZnO nanostructures grown on the seed substrate at low amine:Zn

(0.2:1) concentrations. The presence of multiple peaks indicates the random alignment of the nano structured arrays, consistent with our SEM data. On increasing the amine:Zn concentration, Figures 4c,d,e,f show that the intensity of the (002) plane reflection is increasing relative to other peaks associated with (100) and (101) planes. This indicates that one dimensional nanostructural growth occurs preferentially along the c-axis perpendicular to the substrate. Thus on increasing the amine:Zn up to 1.5:1, the alignment of the ZnO nanorod arrays found to be improved. However, further increasing the amine:Zn concentration to 2:1 (fig 4g) leads to a reduction in this alignment and the emergence of other XRD peaks, especially one associated with the (100) plane. This result shows that the alignment of the nanostructured arrays is strongly influenced by the amine concentration in the growth solution.

In order to study the surface wettability behaviour of the ZnO NR arrays grown at different amine ratios, the water contact angle was evaluated for the different ZnO arrays, as shown in figure 5. Water contact angles from 145° to 36° are obtained for the different amine concentration ratio samples. A sample is considered to be hydrophobic when it has a contact angle greater than 90° and hydrophilic when its contact angle is less than 90° [22]. Figure 5 shows the graph and images of water drops on the surface of the NR arrays grown with different amine concentration ratios. From figure 5, it can be observed that the NR arrays grown at the lowest amine ratios have a contact angle of 83°. On increasing the amine ratio to 1:1 the hydrophobicity increased up to a maximum contact angle of 145°, due to the improvement in NR alignment. At the higher amine concentration ratios the contact angle reduces and the sample changed to a hydrophilic behaviour, due to the irregular growth of micro platelet type structures.

Figure 6 shows PL spectra obtained for ZnO nanostructural arrays measured at 10 K. It is interesting to note that the emission properties of ZnO nanostructured arrays drastically vary with amine concentration. The sample grown at low amine:Zn (0.2:1) concentration ratios show two distinct optical emission features (figure 6a). The emission peak centered at 3.25 eV corresponds to the band edge emission and the broad defect emission peak centered at 2.5 eV originates from defects, most probably due to oxygen vacancies [23, 24]. On increasing the amine:Zn (0.5:1) concentration (figure 6b) the defect emission is suppressed and band edge emission is shifted to 3.2 eV along with the appearance of a blue band emission around 2.9 eV probably associated with Zn interstitials [25]. On further increasing the amine:Zn concentration ratio from 0.75:1 to 2:1 the ratio of Zn interstitial emission at 2.9 eV to band edge emission at 3.2 eV increases (figure 6c,d,e,f). The samples grown at

1.5:1 and 2:1 amine:Zn concentration ratios also both show the broad defect emission centered at 2.5 eV.

The photocatalytic activity of the amine:Zn ratio controlled ZnO NR arrays on glass substrates was investigated using degradation of MB dye. Time dependent UV irradiation shows that the amine ratio controlled ZnO NR arrays are highly active as photocatalysts under UV irradiation. The decomposition efficiency of amine ratio controlled ZnO NR arrays, as well as a bare substrate sample, on MB is shown in figure 7. The sample without ZnO catalyst, shows a decomposition efficiency of 10% of MB dye following UV irradiation for 200 min. In the presence of ZnO NR array catalysts and after UV irradiation of 200 min, the morphology and defect controlled ZnO nanorod arrays exhibited MB decomposition levels of 80%, 88%, 94%, 95%, 96% and 91% of for (0.2:1), (0.5:1), (0.75:1), (1:1), (1.5:1) and (2:1) amine:Zn ratio grown ZnO NRs, respectively. The exponential decay profiles and plots of $\ln(C/C_0)$ versus time suggest that the photodecomposition reactions follow a pseudo-first-order rate law [26]. The calculated rate constant for MB decomposition using these ZnO NR array catalyst samples are 0.007, 0.0136, 0.0155, 0.0163, 0.0182 and 0.0144 min^{-1} for (0.2:1), (0.5:1) 0.75:1), (1:1), (1.5:1) and (2:1) amine: Zn ratio grown ZnO NRs, respectively. These results show that the lowest degradation rate is seen for the sample grown with a (0.2:1) amine:Zn ratio and the sample grown with a (1:1) amine:Zn ratio shows the higher degradation rate.

Previous reports show that amine has a role as a stabiliser which controls the formation of Zn complexes followed by release of Zn (equations 1 to 4) in the growth solution [27] and it also decomposes to form the formaldehyde and ammonia species (equation 5) upon raising the temperature [17]. Reports also show that amine can be an effective surfactant; being a non-polar chelating agent it covers the non-polar planes (100) & (110) of ZnO and thus facilitates the growth of ZnO nanostructures along the [002] axis [11, 28, 29]. J. Cui et al., reported no role due to amine in the growth solution for the growth of ZnO structures via electrodeposition. However in our case, the absence of amine in the growth solution resulted in no formation of ZnO nanostructures and this clearly indicates its active role as a stabiliser for the release of Zn. Table.1 clearly shows the increase in pH of the growth solution observed before and after ZnO NR growth. This may be due to the decomposition of amine into formaldehyde and NH_3. The increase in amine decomposition increases ammonia concentration thereby increasing the pH of the growth solution.

At a low amine:Zn concentration ratio of (0.2:1), a substantial volume of amine decomposes to form ammonia compared to the very small fraction left for the release of Zn for the subsequent formation of ZnO. During NR growth, the amine concentration decreases with time due to decomposition and thus the rate of Zn release also decreases. This can be seen from the SEM images shown previously, where the diameter of NRs grown in these conditions is ~ 200 nm at their base and decreases to 20 nm at the tip. Therefore at lower concentrations, amine behaves a weak stabiliser and only a small fraction of amine is left for ZnO formation. On increasing the amine concentration, a greater fraction of amine is available for ZnO formation and its stabiliser role is promoted. At an amine:Zn concentration ratio of 0.75:1 alignment of the NR arrays is found to be improved and the diameters of the NRs were nearly constant along the length of the NRs, as shown in figure 1c. At an amine:Zn concentration ratio of 1:1 the role of the amine balances between stabilizer and surfactant, resulting in the formation of well aligned, prismatic, NRs with uniform diameters. With further increases of the relative amine concentration, a strong enhancement in the release of Zn in an uncontrolled manner leads to the formation of 2D disc-like structures rather than 1D NR morphologies. In other words, the competition between the stabilizer and surfactant roles of the amine dictates the morphology and alignment of the ZnO NRs.

$Zn(NO_3)_2 + C_6H_{12}N_4 \rightarrow [Zn(C_6H_{12}N_4)]^{2+} + 2NO_3^-$ .....…..(1)

$[Zn(C_6H_{12}N_4)]^{2+} + 4OH^-$ ---------- $Zn(OH)_4^{2-} + C_6H_{12}N_4$…….(2)

$Zn(OH)_4^{2-}$ ----------$Zn^{2+} + 4OH^-$ ……..(3)

$Zn^{2+} + 2OH^-$ ------ $Zn(OH)_2$----------$ZnO + H_2O$ ……..(4)

$C_6H_{12}N_4 + 6H_2O \leftrightarrow 6CH_2O + 4NH_3$ ..... (5)

It is interesting to note, along with morphology and alignment, that the emission properties of ZnO nanostructured arrays also vary with their morphology. Our data provides evidence that the relative amine concentration plays a role in controlling the optically active defect concentration in ZnO NRs in addition to controlling the NR morphology and alignment. PL analysis revealed that the sample grown at a low amine:Zn concentration ratio had a dominant defect emission peak centered at 2.5 eV, probably due appearance of a strong green emission is ascribed to the formation of oxygen

vacancy defects or antisite defects (OZn). On increasing the amine:Zn concentration ratio, the oxygen vacancy defect emission was found to be suppressed and a new defect emission around 2.9 eV (probably associated with Zn interstitials) emerges accompanied by change in the detailed spectral shape of the band edge emission (3.25 eV). This increase in Zn interstitial defects as a function of amine concentration may be attributed to a greater release of Zn in the growth solution associated with enhancement of the 'stabiliser' role of the amine. The low temperature PL spectrum for samples with different amine concentration ratios were shown in the figure 6. The fitted peak position of the FX emission varied from 3.38eV to 3.31 eV as the hexamine concentration was increased from (0.2:1) to (1.5:1) ratio. It is possible that the defect density is responsible for the increase in carrier concentration on the ZnO nano arrays. Due to the presence of the high defect density, the FX emission was totally suppressed in the micro structure arrays grown in high amine ratio. The interesting fact is that on controlling the amine ratio in the growth solution, the domination of free excitonic emission was varied. As stated previously, the additional low intensity peak at ~ 2.9 eV has been associated with a transition between a state due to Zn interstials and the valence band [25]. This association is consistent with our data because the increased Zn interstitial concentration may be due to the increasing Zn release rate with increasing amine concentration in the growth solution.

The mechanism behind photocatalytic activity on metal oxides is based on electrons (e-) and holes (h+) creation upon irradiating the nanocatalysts. When the incident photon energy exceeds the band gap energy of the nanomaterial, electron-hole pairs are created. These photoexcited electron-hole pairs reach the surface of the nanoparticles and generate reactive oxygen species (ROS) which is responsible for degradation of the dye solution [30]. When aqueous ZnO suspension is illuminated by UV light the conduction band electrons (e-) and valence band holes (h+) are generated. Majority of the photoexcited electron-hole pairs recombine before reaching to nanocatalyst surface. Surface defects play a vital role on the enhancement of photocatalyst activity. Oxygen vacancies in ZnO nanoparticles act as a trap states for photogenerated electrons or holes which prevent the recombination and enhances the photocatalytic activity [31]. In our case, PL spectra clearly exhibit that on increasing the amine ratio, zinc interstitial defects were increased (Figure.6). The influence of zinc interstitials in ZnO nanostructures on the photocatalytic performance is not understood sofar. Zinc interstitials are shallow donors lie 0.26 eV below the conduction band of ZnO [32-35] readily supply electrons to conduction band and increases the carrier concentration at the surface of nanostructures. Increase in carrier concentration at the surface could lead the formation of space

charge region near to the nanocatalayst surface [36]. The space charge region could affect energy band structure and local conductivity at nanocatalyst surface. The space charge formation due to the accumulation of electrons at nanocatalyst surface may cause downward band bending associated with the interfacial electric field in the space charge region as shown in the schematics (Figure. 8) which may facilitate the separation of photogenerated electrons and holes and thus enhances the photocatalytic behavior. Our results showed that the density of the nanostructures grown at low amine:Zn concentration ratio (0.2:1) is around 12 NRs/μm^2 (Figure. 1) whereas the samples grown in amine:Zn concentration ratio (0.5:1) to (1.5:1) show higher density in the range of ~ 56 NRs/ μm^2 (Figure.1). ZnO nanostructures fabricated at low amine concentration show slower photocatalytic response due to lower density of ZnO nanostructures. On increasing the amine:Zn concentration ratio (0.5:1)-(1.5:1), the photocatalytic degradation efficiency found to be enhanced with the increase of Zn interstitials. The micron scale platelets grown at high amine ratio (2:1) exhibit slow photocatalytic degradation due to their low surface to volume ratio.

Conclusions

We have demonstrated that the morphology, alignment and optically active defect content of vertically aligned 1D ZnO NR arrays grown using an aqueous solution method can be controlled by simply varying the hexamine relative concentration in the growth solution. Well aligned, prismatic ZnO NR arrays with a uniform NR diameter of 80 nm along their lengths were obtained at an amine:Zn ratio of 1:1. We propose that amine concentration not only plays an important role on the growth and alignment of the 1D NR arrays, but it also plays a role in controlling their optically active defect concentration. Amine plays a role both as growth stabilizer and as a surfactant and thus controls the Zn release rate for ZnO formation while also capping non polar planes. The competition between these 'stabliser' and 'surfactant' roles facilitates the morphology, alignment and defect control of 1D ZnO NR arrays. These defect controlled NR arrays have also been demonstrated to work as effective photocatalysts and exhibit excellent photocatalytic activity under UV irradiation. ZnO NR arrays grown at amine concentrations of 1M show higher photocatalytic degradation in an MB dye solution under UV irradiation owing to both the high surface to volume ratio of the arrays and increased charge carrier density due to Zn interstitial defects. Understanding and then utilizing the role of amine in the growth of 1D ZnO NR arrays offers tremendous promise as a simple but highly effective method for tailoring ZnO NR morphologies (and thus functionalities) for various potential applications.

Acknowledgements

The authors KSR and RTR would like to thank the Department of Science and Technology, Government of India, for financial support under the Nano mission project (SR/NM/NS-113/2010-BU (G)) and the authors EMCG, KSR and RTR would like to thank both Dublin City University and the Department of Science and Technology, Government of India, for financial support, including travel funding, under the Indo-Ireland bilateral project (DST/INT/IRE/P-16/2011).

References

1. Sheng Xu; and Zhong Lin Wang. Nano Research. 2011, 4, 1013-1098.
2. F. Fang; J. Futter; A. Markwitz; J. Kennedy. Nanotechnology. **2009**, 20,245502.
3. Charu Dwivedi; V Dutta. Adv. Nat. Sci.: Nanosci. Nanotechnology. **2012**, 3,015011.
4. R. Konenkamp; R. C. Word; M. Godinez. Nano Letters. **2005**, 5, 2005-2008.
5. Michael S. Arnold; Phaedon Avouris; Zheng Wei Pan; Zhong L. Wang. J. Phys. Chem. B. **2003**, 107, 659-663.
6. Zengxing Zhang; Huajun Yuan; Jianjun Zhou; Dongfang Liu; Shudong Luo; Yanming Miao; Yan Gao; Jianxiong Wang; Lifeng Liu; Li Song; Yanjuan Xiang; Xiaowei Zhao; Weiya Zhou; Sishen Xie. J. Phys. Chem. B. **2006**, 110, 8566-8569.
7. R. T. Rajendra Kumar; E. McGlynn; M. Biswas; R. Saunders; G. Trolliard; B. Soulestin; J.-R. Duclere; J. P. Mosnier; M. O. Henry; J. Appl. Phy. **2008**, 104, 084309.
8. Elena Galoppini; Jonathan Rochford; Hanhong Chen; Gaurav Saraf; Yicheng Lu; Anders Hagfeldt; Gerrit Boschloo. J. Phys. Chem. B. **2006**,110, 16159-16161.
9. Guozhen Shen; Yoshio bando; Baodan Liu; Dmtri Golberg; Cheol Jin Lee. Adv. Funct. Mater. **2006**, 16, 410-416.
10. Ye Sun; Gareth M. Fuge; Michael, N.R; Ashfold. Chemical Physics Letters. **2004**, 396, 21-26.
11. Jingbiao Cui. J. Phys. Chem. C. **2008**, 112, 10385-10388.
12. Francisco Solís-Pomar; Eduardo Martínez; Manuel F Meléndrez; Eduardo Pérez-Tijerinal. Nanoscale Research Letters. **2011**, 6,524.
13. Yong-Jin Kim; Chul-Ho Lee; Young Joon Hong; Gyu-Chul Yi. Appl. Phys. Letters. **2006**, 89, 163128.
14. B. Angadi; H. C. Park; H. W. Choi; J. W. Choi; W. K. Choi. J. Phys. D: Appl. Phys. **2007**, 40, 1422-1425.
15. J. Lee; J. Chung; S. Lim. Physica E. **2010**, 42, 2143-2146.

16. X. Q. Zhao; C. R. Kim; J. Y. Lee; C. M. Shin; J. H. Heo; J. Y. Leem; H. Ryu; J. H. Chang; H. C. Lee; C. S. Son; B. C. Shin; W. J. Lee; W. G. Jung; S. T. Tan; J. L. Zhao; X. W. Sun. Appl. Surf. Science. **2009**, 255, 5861-5865.
17. Tz-Jun Kuo; Chun-Neng Lin; Chi-Liang Kuo; Michael H. Huang. Chem. Mater. **2007**, 19, 5143-5147.
18. Tianjun Sun; Jieshan Qiuand; Changhai Liang. J. Phys. Chem. C. **2008**, 112, 715-721.
19. Jiu-Ju Feng; Zhen-Zhen Wang; Yong-Fang Li; Jian-Rong Chen; Ai-Jun Wang; J Nanopart Res. **2013**, 15,1565.
20. K. S. Ranjith; S. Pandian; N. Gomathi; M. Kamruddin; R. T. Rajendrakumar. Advanced Material Research. **2012**, 584, 319-323.
21. C. Sahoo; A. K. Gupta; A. Pal. Desalination. **2005**, 181, 91-100.
22. http://phys.org/news/2013-07-hydrophobic-hydrophilic.html
23. Yang Zhang; Manoj, K. Ram; Elias K. Stefanakos; D. Yogi Goswami. Journal of Nanomaterials. **2012**, 2012**,** 624520.
24. Zeng xing Zhang; Huajun Yuan; Jianjun Zhou; Dongfang Liu; Shudong Luo; Yanming Miao; Yan Gao; Jianxiong Wang; Lifeng Liu; Li Song; Yanjuan Xiang; Xiaowei Zhao; Weiya Zhou; Sishen Xie. J. Phys. Chem. B. **2006**, 110, 8566-8569.
25. R.N. Gayen; A. Rajaram; R. Bhar; A.K. Pal. Thin Solid Films. **2010**, 518, 1627-1636.
26. Behnajady MA; Modirshahla N; Hamzavi R. J Hazard Mater. **2006**, 133, 226-232.
27. Mohamad Hafiz Mamat; Zuraida Khusaimi; Musa Mohamed Zahidi; Suriani Abu Bakar; Yosri Mohd Siran; Syahril Anuar MdRejab; Ahmad Jaril Asis; ShawaluddinTahiruddin; Saifollah Abdullah; Mohamad Rusop Mahmood. Jpn. J. Appl. Phys. **2011**, 50, 06GH04.
28. A. Suguna; HC. Warad; M. Boman; J. Dutta. J. Sol-Gel Technology. **2004**, 39, 49-56.
29. R. A. Laudise; E. D. Kolb; A. J. Caporaso. **1964**, 47, 9-12.
30. Yang Li, Wen Zhang, Junfeng Niu, Yongsheng Chen; ACS Nano. **2012**, 6, 5164–5173.
31. Jianchun Wang, Ping Liu, Xianzhi Fu, Zhaohui Li, Wei Han, Xuxu Wang; *Langmuir*. **2009**, 25, 1218-1223.
32. Christoph Knies, Matthias T. elm, Peter J. Klar, Jan Stehr, Detlev M. Hofmann, Nikolai Romanov, Tom Kammermeier, Andreas Ney; Journal of Applied Physics. **2009**, 105, 073918.
33. J.Sann, J.Stehr, A.Hofstaetter, D.M.Hofmann, A.Neumann, M.Lerch, U.Haboeck, A.Hoffmann, C.Thomsen; Physical Review B. **2007**, 76, 195203.
34. Aleksandra B.Djurisic and Yu Hand Leung; Small. **2006**, 2, 944-961.

35. M.Trunk, V.Venkatachalapathy, A. Galeckas, A.Yu. Kuznetsov; Applied Physics Letter. **2010**, 97, 211901.

36. Zhen Zhang, John T.Yates; Chemical Reviews. **2012**, 112, 5520-5551.

Table

Table I: Growth parameters, pH, diameter and length of ZnO nanostructures grown with different amine:Zn concentrations.

S. No	Amine Ratio (Hexamine: Zinc Nitrate)	Growth initial pH	Growth ending pH	Average Diameter	Length
1	0.2:1	5.10	6.17	.....	~1μm
2	0.5:1	5.24	6.45	~30nm	~1μm
3	0.75:1	5.47	6.68	~50nm	~400nm
4	1:1	5.63	6.93	~60nm	~400nm
5	1.5:1	5.71	7.26	~100nm	~150nm
6	2:1	5.82	7.94	.....	.....

Figure Caption

Figure 1: SEM images showing plan views of ZnO nanostructure arrays grown on dip coated ZnO thin film seeded substrates at amine: zinc nitride ratios of (a) 0.2:1, (b)0.5:1, (c)0.75:1, (d) 1:1, (e) 1.5:1, (f) 2:1. The images in the insets are more highly magnified images of the respective nanostructures shown in the main images.

Figure 2: Schematic diagram of the nanostructured arrays grown with different amine:zinc nitride concentrations of (a)0.2:1, (b)0.5:1, (c)0.75:1, (d)1:1, (e) 1.5:1, (f) 2:1.

Figure 3: SEM image showing cross sectional views of 1D NR arrays grown on dip coated ZnO thin film seeded substrates with amine:zinc nitride ratios of (a) 0.2:1, (b) 1:1 , (c) 1.5:1. Schematic representations of the morphologies with varying amine:zinc nitrate ratios are also shown in (d)0.2:1, (e) 1:1, (f) 1.5:1.

Figure 4: XRD patterns from nanostructured arrays grown using different amine:zinc nitrate concentrations (a)standard pattern of ZnO (JCPDS 36-1451), (b)0.2:1, (c)0.5:1, (d)0.75:1, (e)1:1, (f) 1.5:1, (j) 2:1.

Figure 5: Water contact angle on ZnO NR arrays as a function of varying the amine concentration ratio.

Figure 6: PL spectra (measured at 10 K) of ZnO nanostructured arrays grown with different hexamine:zinc nitrate concentrations (a) 0.2:1, (b) 0.5:1, (c) 0.75:1, (d) 1:1, (e) 1.5:1, (f) 2:1. Insets show the corresponding sample morphologies.

Figure 7: (a) The photo degradation efficiency of MB versus time using ZnO NR array samples grown with hexamine:zinc nitrate concentrations of 0.2:1, 0.5:1, 0.75:1, 1:1,1.5:1 and 2:1. (b) Kinetics of photocatalytic degradation of MB in the presence of ZnO NR array samples grown with different hexamine:zinc nitrate concentrations.

Figure 8: Schematic diagram showing the energy levels and free charge carrier densities from the ZnO nanostructural surface to the dye solution (a) under dark and (b) under UV irradiation.

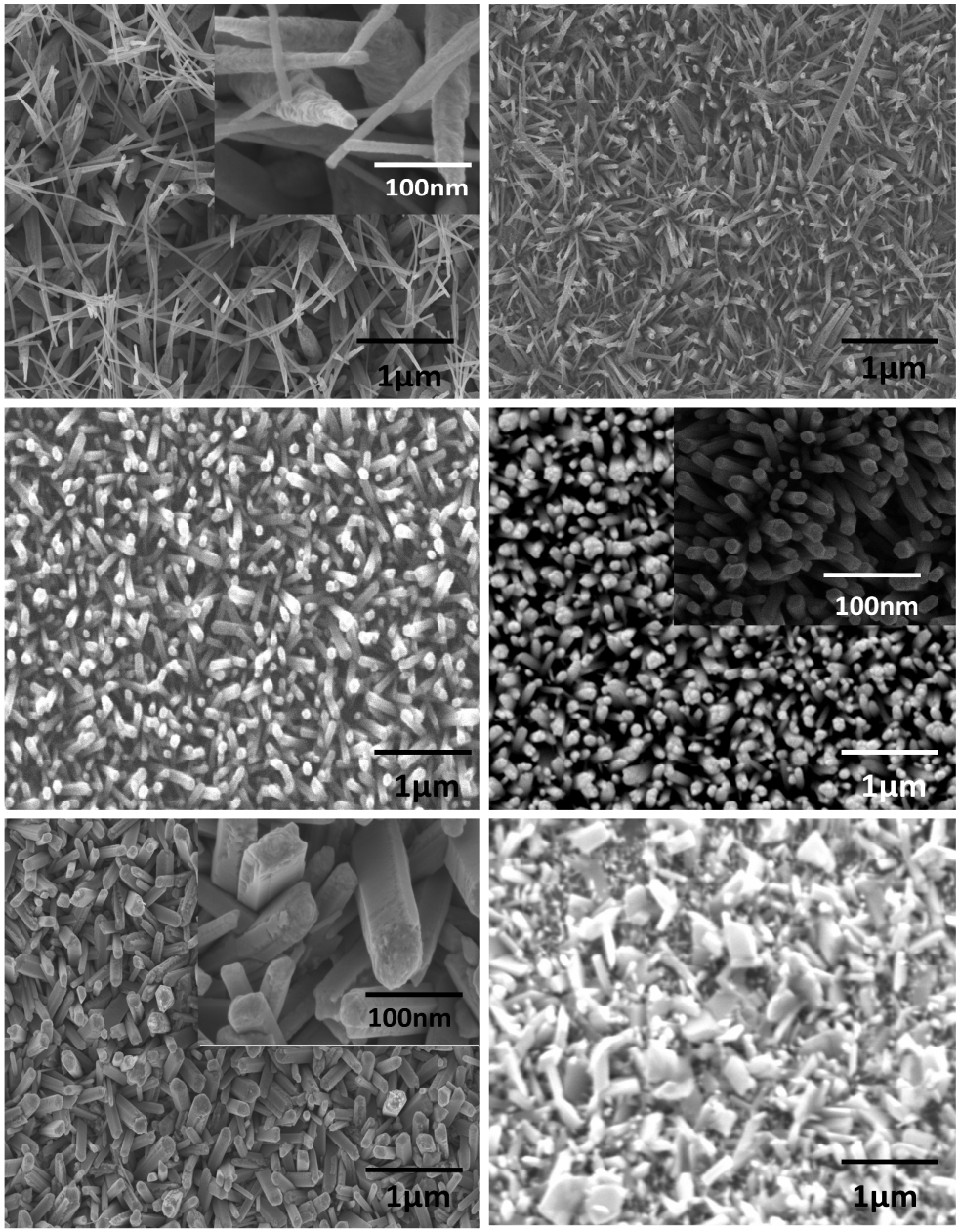
100nm
1µm
1µm
1µm
100nm
1µm
100nm
1µm
1µm

Figure 1

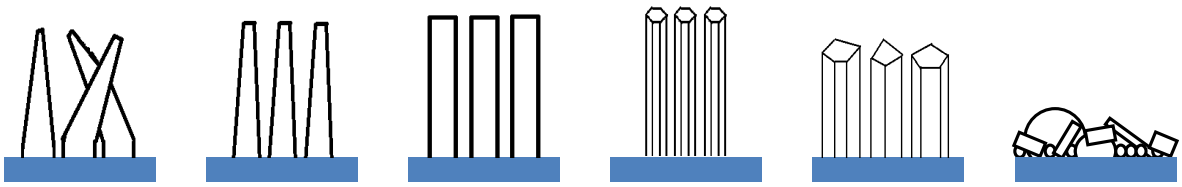

Figure 2

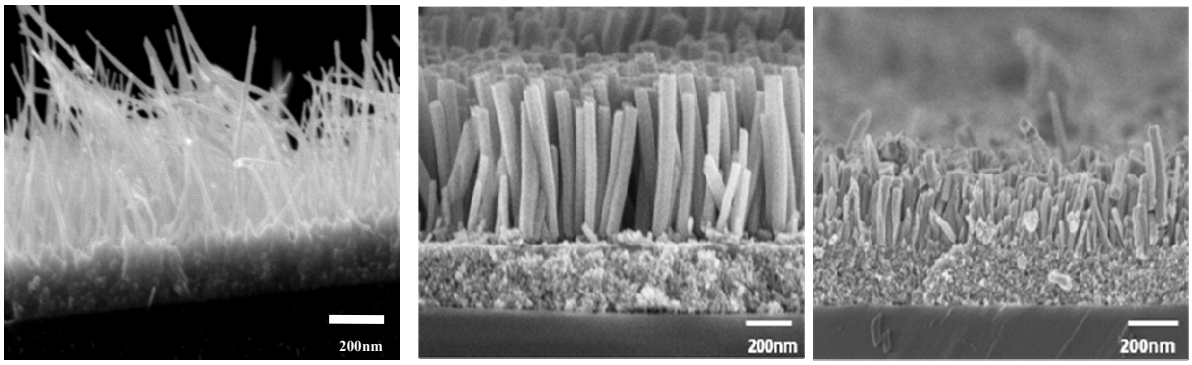

Figure 3

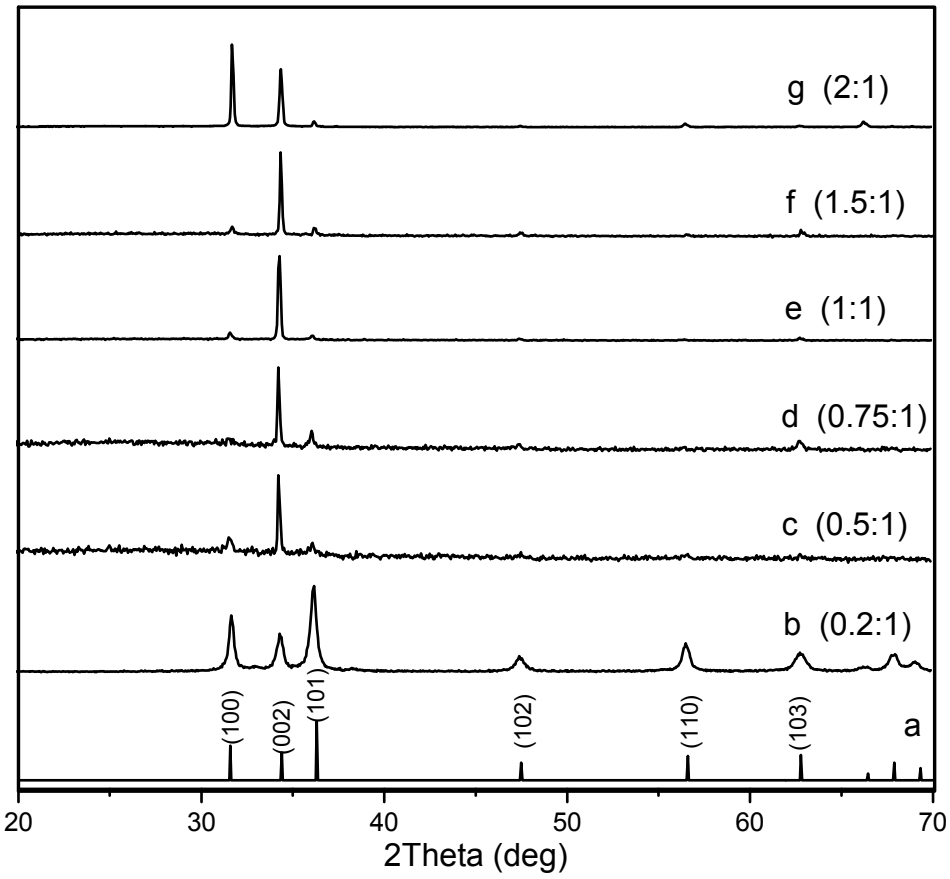

Figure 4

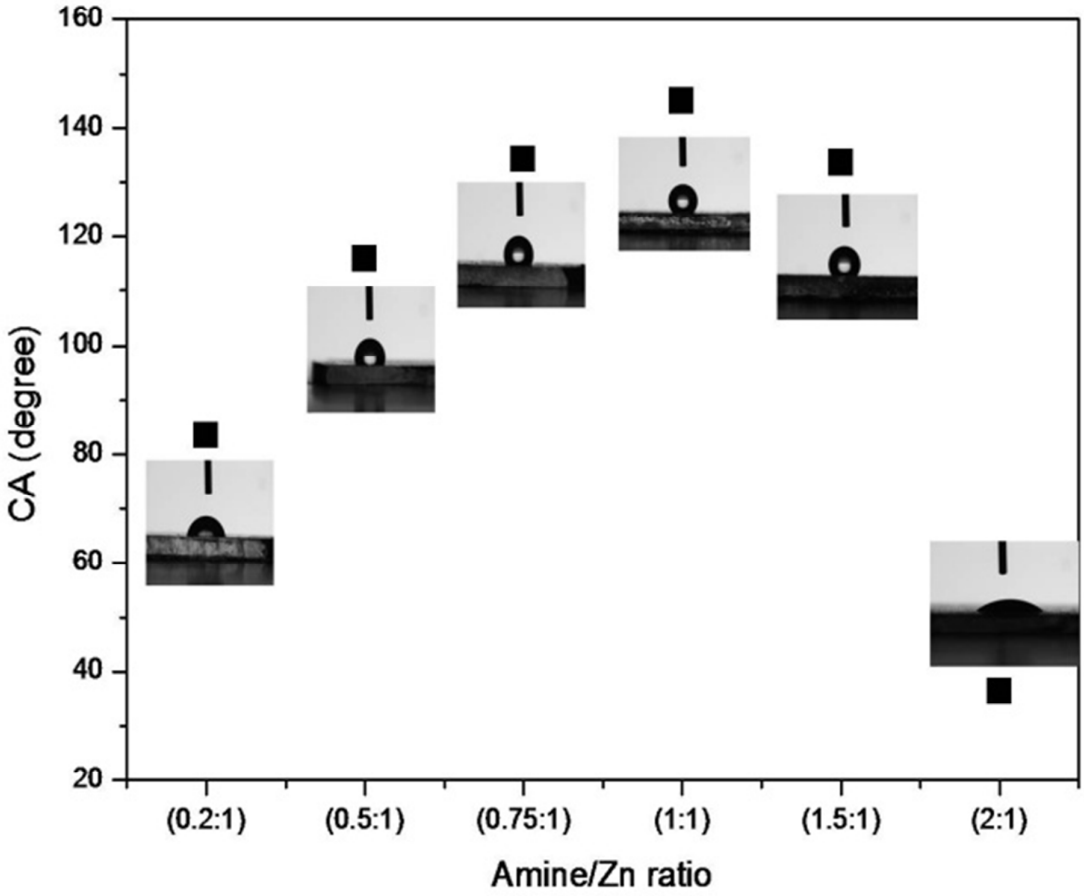
160
140
120
100
80
60
40
20
CA (degree)
(0.2:1)
(0.5:1)
(0.75:1)
(1:1)
(1.5:1)
(2:1)
Amine/Zn ratio

Figure 5

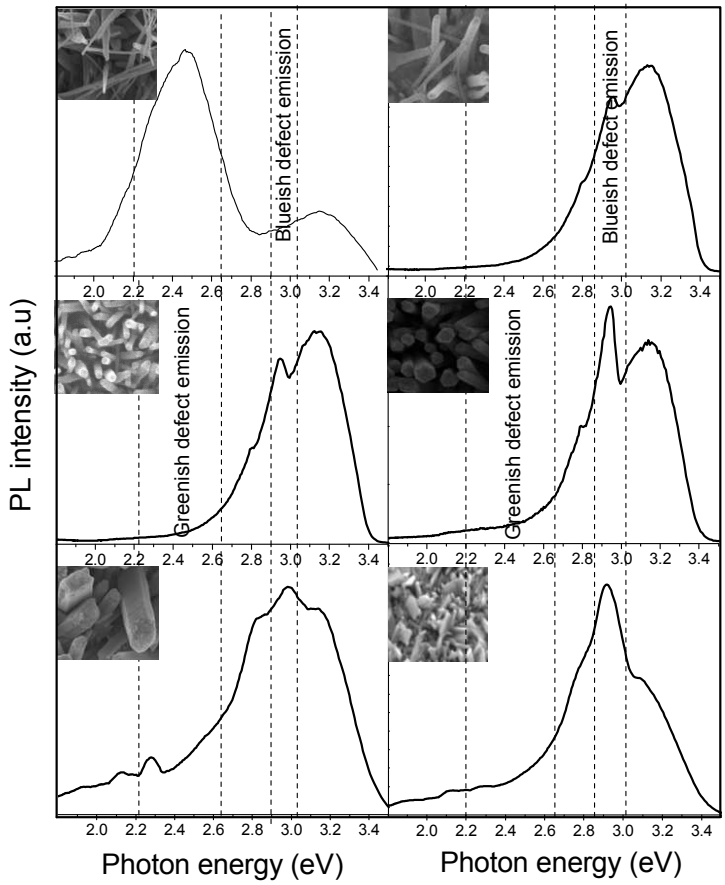
Blueish defect emission
Greenish defect emission
PL intensity (a.u)
2.0 2.2 2.4 2.6 2.8 3.0 3.2 3.4
Photon energy (eV)

Figure 6

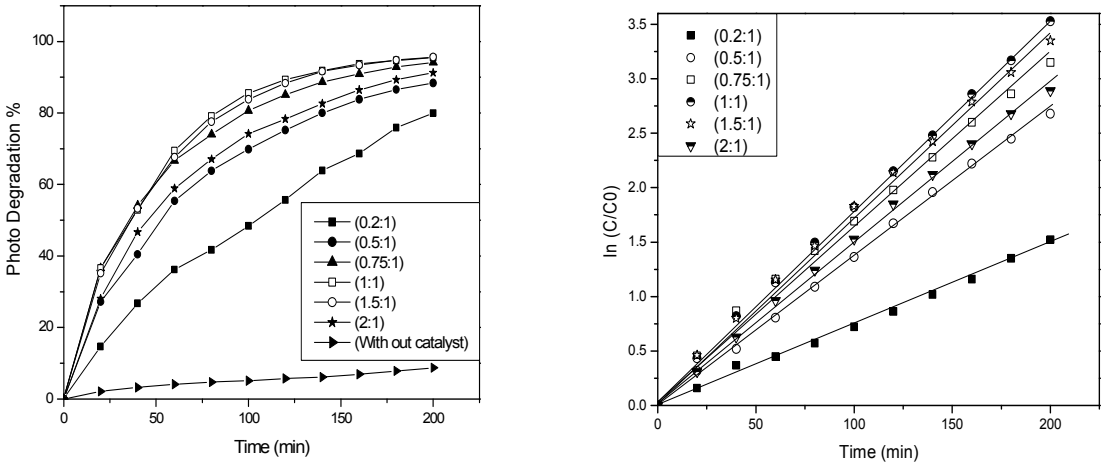

Figure 7

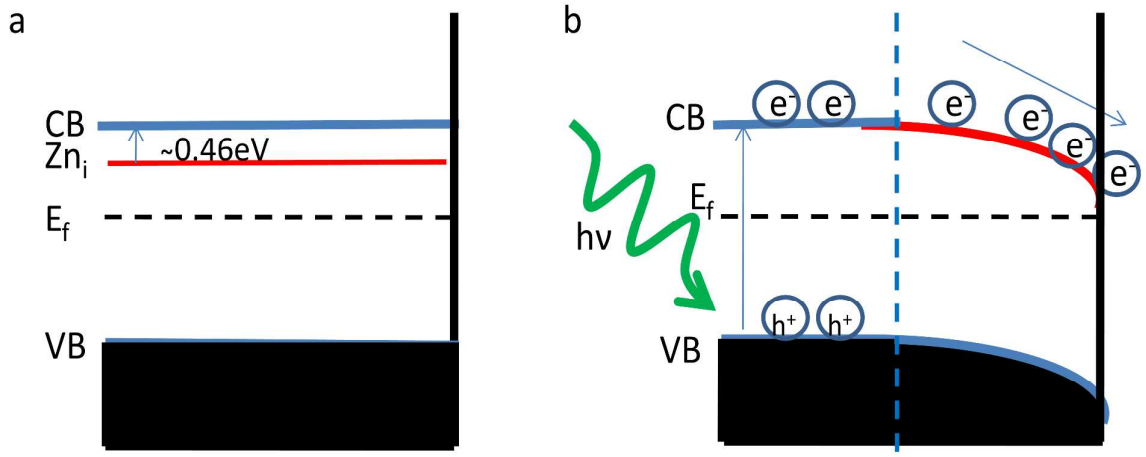

Figure 8

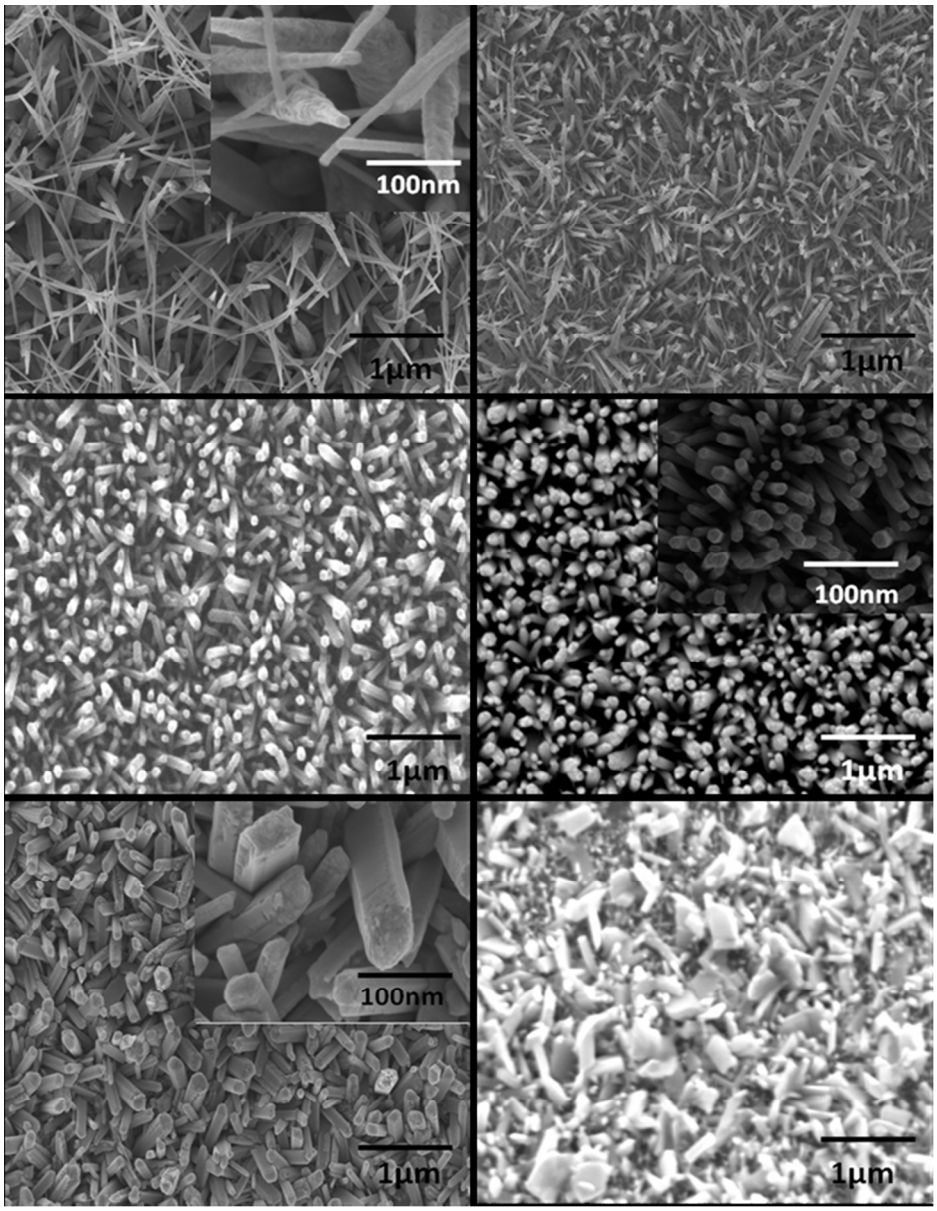

SEM images showing plan views of ZnO nanostructure arrays grown on dip coated ZnO thin film seeded substrates at amine: zinc nitride ratios of (a) 0.2:1, (b)0.5:1, (c)0.75:1, (d) 1:1, (e) 1.5:1, (f) 2:1. The images in the insets are more highly magnified images of the respective nanostructures shown in the main images.
136x177mm (150 x 150 DPI)

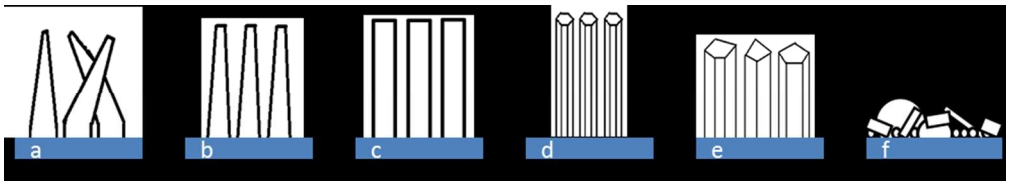

Schematic diagram of the nanostructured arrays grown with different amine:zinc nitride concentrations of (a)0.2:1, (b)0.5:1, (c)0.75:1, (d)1:1, (e) 1.5:1, (f) 2:1.
167x29mm (150 x 150 DPI)

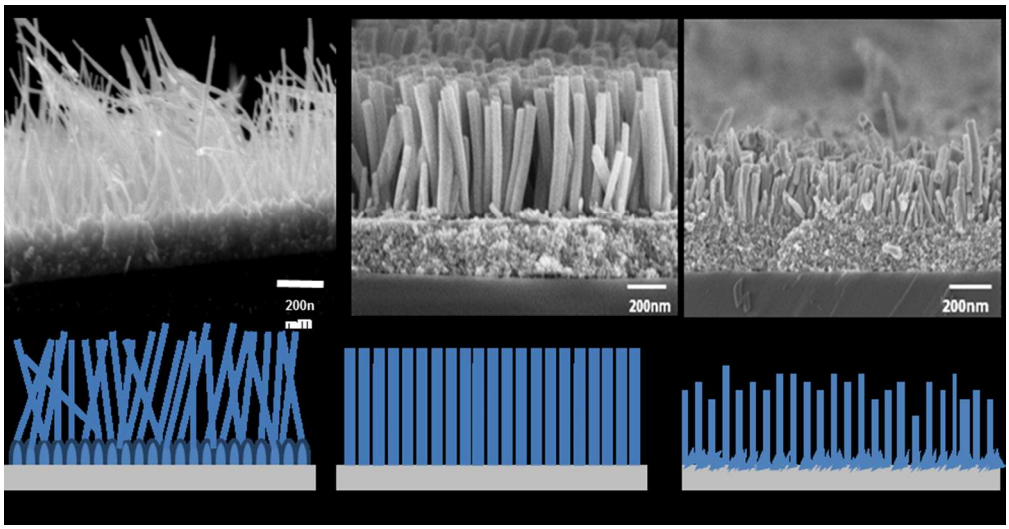

SEM image showing cross sectional views of 1D NR arrays grown on dip coated ZnO thin film seeded substrates with amine:zinc nitride ratios of (a) 0.2:1, (b) 1:1 , (c) 1.5:1. Schematic representations of the morphologies with varying amine:zinc nitrate ratios are also shown in (d)0.2:1, (e) 1:1, (f) 1.5:1.
167x86mm (150 x 150 DPI)

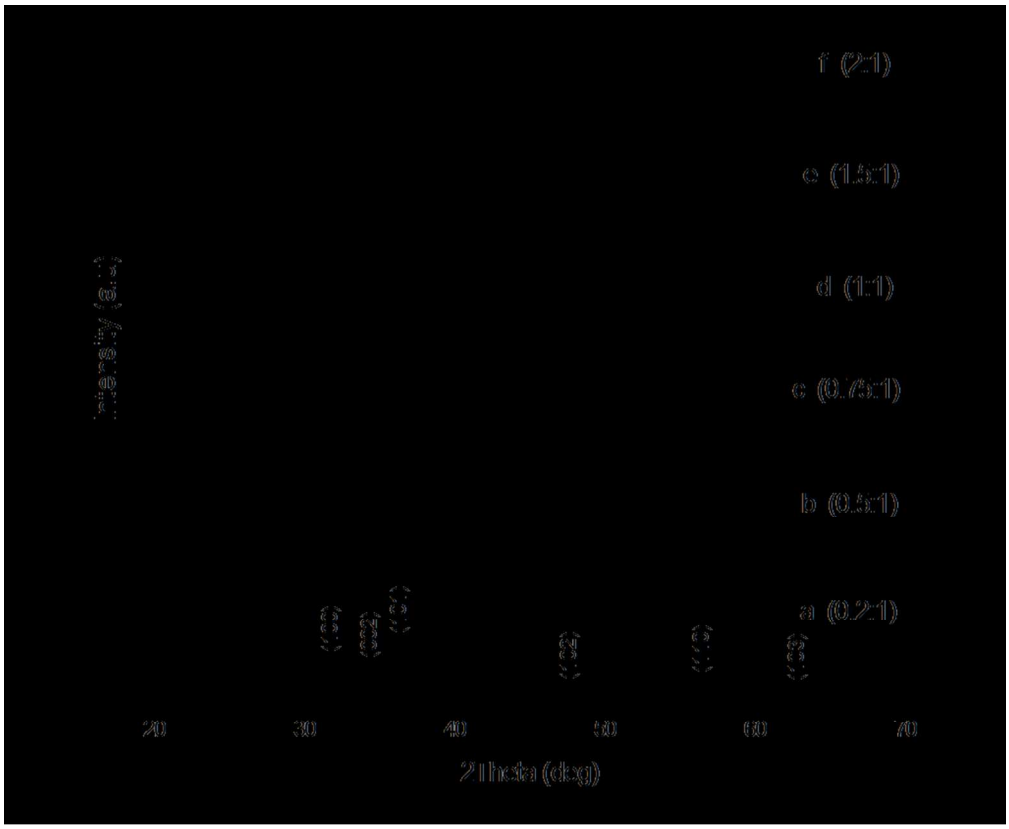

XRD patterns from nanostructured arrays grown using different amine:zinc nitrate concentrations (a)0.2:1, (b)0.5:1, (c)0.75:1, (d)1:1, (e) 1.5:1, (f) 2:1.

172x141mm (150 x 150 DPI)

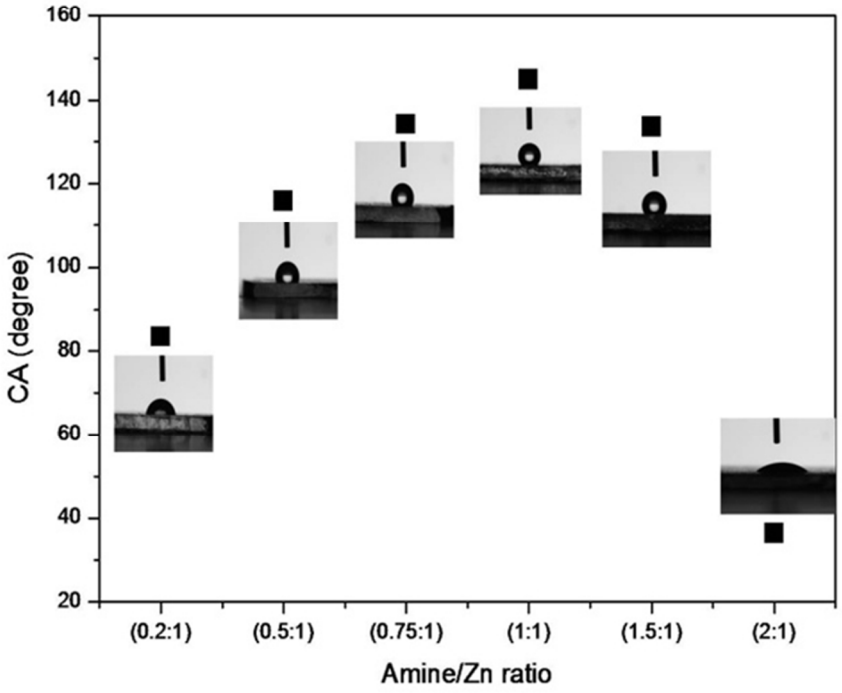

Water contact angle on ZnO NR arrays as a function of varying the amine concentration ratio.
182x155mm (104 x 104 DPI)

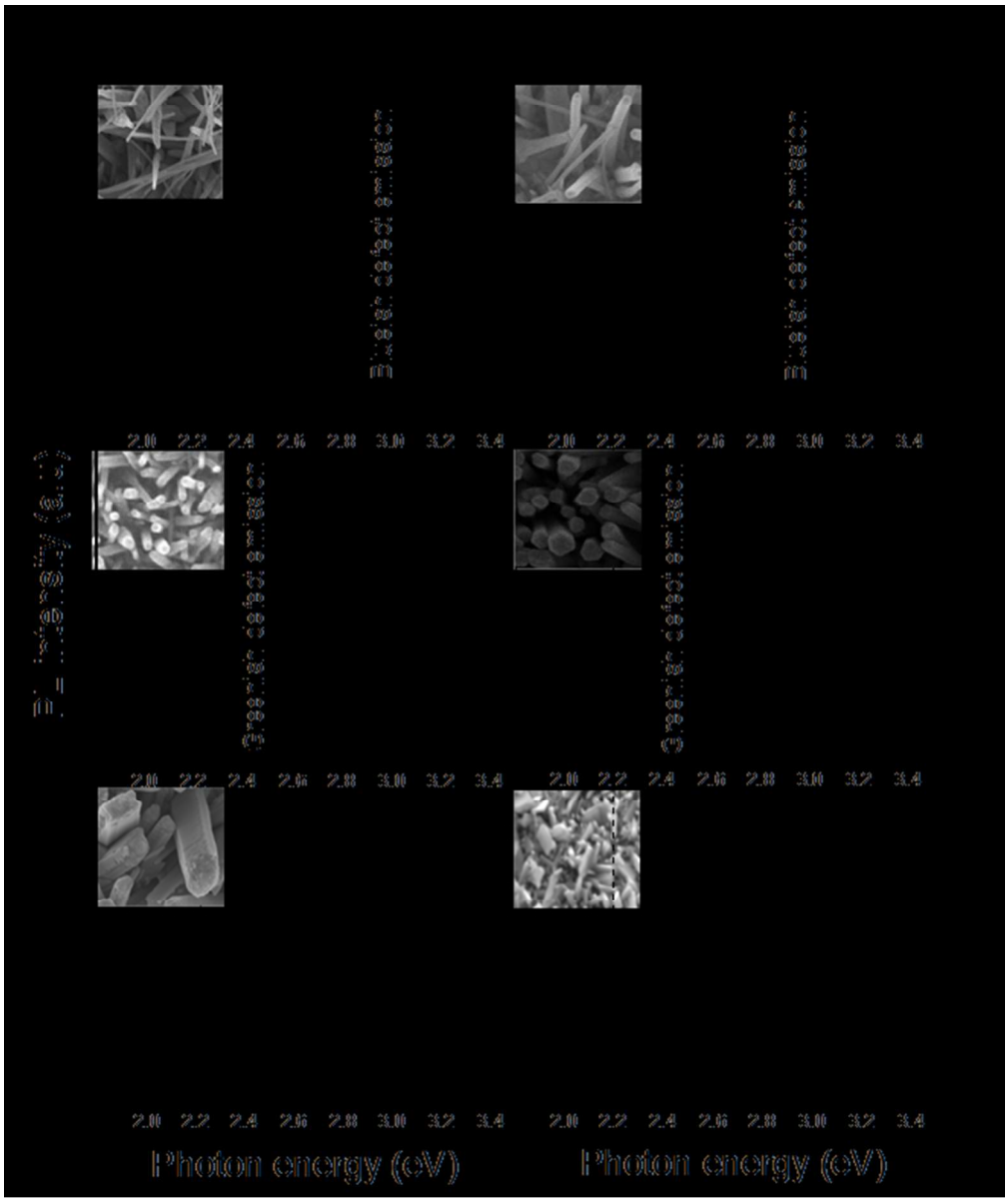

PL spectra (measured at 10 K) of ZnO nanostructured arrays grown with different hexamine:zinc nitrate concentrations (a) 0.2:1, (b) 0.5:1, (c) 0.75:1, (d) 1:1, (e) 1.5:1, (f) 2:1. Insets show the corresponding sample morphologies.
111x132mm (150 x 150 DPI)

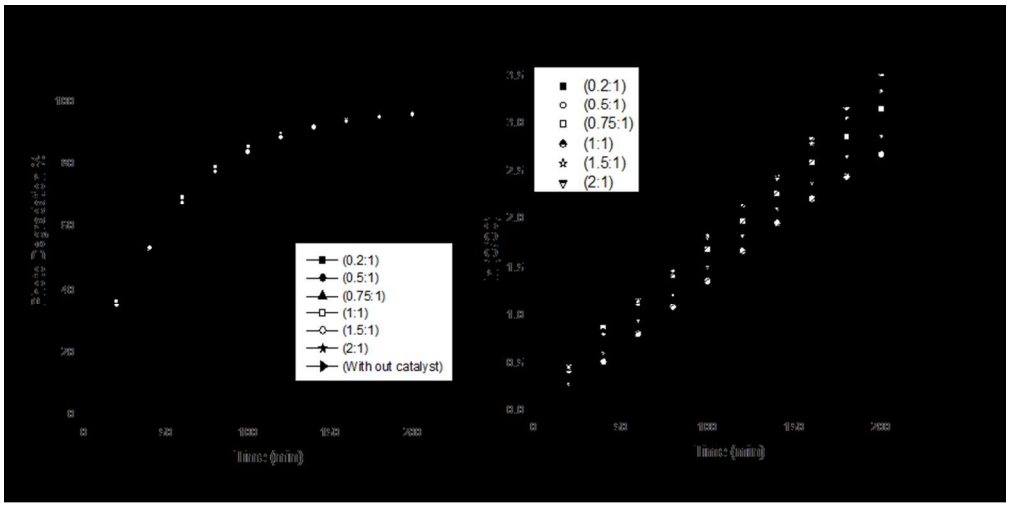

(a) The photo degradation efficiency of MB versus time using ZnO NR array samples grown with hexamine:zinc nitrate concentrations of 0.2:1, 0.5:1, 0.75:1, 1:1,1.5:1 and 2:1. (b) Kinetics of photocatalytic degradation of MB in the presence of ZnO NR array samples grown with different hexamine:zinc nitrate concentrations.
159x79mm (150 x 150 DPI)

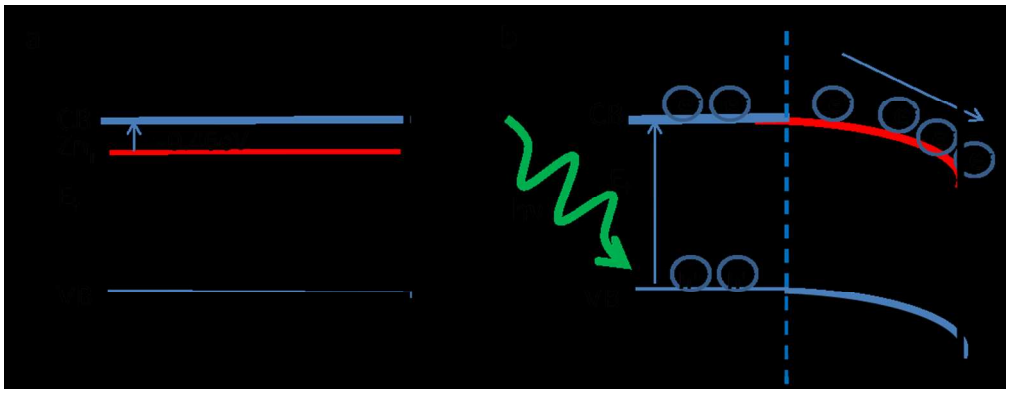

Schematic diagram showing the energy levels and free charge carrier densities from the ZnO nanostructural surface to the dye solution (a) under dark and (b) under UV irradiation.
195x75mm (150 x 150 DPI)